Fermilab

TM-1389
0401.000

MEASUREMENT OF THE MAIN RING LONGITUDINAL IMPEDANCE BY DEBUNCHING

K.-Y. Ng

February 1986

MEASUREMENT OF THE MAIN RING LONGITUDINAL IMPEDANCE BY DEBUNCHING

King-Yuen Ng

February 1986

I. INTRODUCTION

An experiment was carried out by Jim Crisp[1] to observe microwave signals of the bunched beam in the Fermilab Main Ring. The purpose of this paper is to analyze the experiment and attempt a computation of the longitudinal impedance per unit harmonic Z/n of the Main Ring. The result of the analysis indicates $Z/n = 8.6\ \Omega$ if the driving impedance is a broad band at $f_{MW} = 1.646$ GHz. However, if the driving impedance is a high-Q resonance at 1.646 GHz with RMS width less than ~0.13 GHz (or $Q \gtrsim 50$), Z_{sh}/Q of the resonance is 5.2 kΩ.

In Section II, the experiment is briefly reviewed. In Section III, we demonstrate that the proton bunches are of Gaussian shape. In Section IV, the time at which the microwave amplitude starts to grow is determined. We find that this occurs when two adjacent bunches overlap each other. A stability criterion is derived for the overlapped bunches in Section V. Then Z/n and Z_{sh}/Q are computed. Finally in Section VI, the source of the driving impedance is traced and some discussions presented.

II. THE EXPERIMENT

The method of debunching[2] is used in the experiment to generate microwave signals. Nine bunches each of intensity $N = 0.636 \times 10^{10}$ protons were accelerated to 150 GeV. Each bunch had a bunch area (95%) of 0.231 eV-sec sitting in a h = 1113 RF bucket with RF voltage equal to 1.079 MV. The RF voltage was turned off suddenly. The bunches tended to shear. As the energy spread became smaller and smaller, Landau damping failed and microwave signals started to grow.

A coaxial directional coupler designed by Jim Griffin[3] was used to pick up the microwave signals. The detector consists of two concentric pipes a quarter wavelength long having a characteristic impedance of 12.5 ohms. Each end has four symmetrically spaced 50 ohm ports. The signals were transported from the enclosure via a 177 nsec long 7/8" heliax cable. A spectrum analyzer in zero-span mode was used to monitor the amplitude of the 31st harmonic of the h = 1113 RF frequency (f_{MW} = 1.646 GHz). Zero-span mode basically plots the amplitude of the signal that passes through an equivalent filter with the center frequency and bandwidth specified. The peak detector was not used because it has the disadvantage that the signal must overcome the diode forward voltage drop before it can

be detected, whereas the spectrum analyzer has a linear response to small signals and a logarithmic scale. The photos in Figure 1 compare the displays of the spectrum analyzer and peak detector for a typical run. The diode detector indicates a time of 60 msec for the onset of the microwave growth but the analyzer shows a clear minimum at about 30 msec.

III. BUNCH SHAPE

Figure 2 shows the bunch shape in the last few turns before the RF voltage was turned off. A typical bunch shape is selected and is fitted by a Gaussian curve with RMS time spread $\hat{\sigma}_\tau$ and also a parabolic curve with maximum half spread $\hat{\tau}$. The results are: for Gaussian, $\hat{\sigma}_\tau$ = 0.635 ns with ERROR = 0.0035 and, for parabolic $\hat{\tau}$ = 1.278 ns with ERROR = 0.0299. Here, the error of each fitting is determined by

$$ERROR = \frac{\int [f_F(\tau) - f_E(\tau)]^2 d\tau}{\int f_E(\tau) d\tau}, \tag{3.1}$$

where f_F and f_E represent the fitted and experimental bunch shapes respectively. The fittings are displayed in Figure 3. The frequency response of the detector to a 30 psec electron bunch is shown in Figure 4. We see that the response is relatively flat and rolls off after 2 GHz. We believe that the bunch shape would not be distorted very

much by the detector. The result of the fittings shows clearly that the bunch is relatively Gaussian in shape with RMS spread $\hat{\sigma}_\tau$ = 0.635 ns. The RF voltage was 1.074 MV. This leads to a RMS energy spread of $\hat{\sigma}_E$ = 0.0192 GeV and an emittance of $6\pi\hat{\sigma}_\tau\hat{\sigma}_E$ = 0.230 eV-sec.

IV. DETERMINATION OF STARTING TIME OF MICROWAVE GROWTH

It is tempting to identify the start of microwave instability to be t_o ~30 msec when the microwave amplitude in Figure 1(a) reaches a minimum. In fact, the growth may start well before that time. Since our bunch is Gaussian in shape, a dispersion relation at time $t = t_o(1+x)$ after the RF is turned off can be written in the closed form (see derivation in Appendix I),

$$1 + ia(1+x)\left[1 - i\sqrt{\pi}\,u\,w^*(u)\right] = 0, \qquad (4.1)$$

where w(u) is the complex error function,

$$u = \frac{\Delta\Omega}{\sqrt{2}\,n\,\sigma_\omega}, \qquad (4.2)$$

and

$$a = \frac{Z}{n}\frac{eNt_0}{(2\pi)^{3/2}\hat{\sigma}_\tau^{\,2}\hat{\sigma}_E} \quad . \qquad (4.3)$$

In above, $\Delta\Omega$ is the coherent frequency shift ($\mathrm{Im}(\Delta\Omega)>0$ implies a growth), σ_ω the RMS revolution frequency spread of the bunch at time $t = t_o(1+x)$, $\hat{\sigma}_T$ and $\hat{\sigma}_E$ the RMS time and energy spreads before the RF is turned off, e the electric charge of the proton, N the number of protons per bunch, and Z/n the longitudinal impedance per harmonic driving the growth. At the threshold, $x = 0$, solution of Eq. (4.1) gives $\mathrm{Re}(u) = 0.92414$ and $\mathrm{Im}(u) = 0$. Thus $a = 1.4341$. Therefore from Eq. (4.3), Z/n can be evaluated once t_o is known.

Solving Eq. (4.1) numerically, the power growth of the amplitude from $A(t_o)$ to $A(t_o(1+x))$ can be written as

$$\ln \left| \frac{A(t_o(1+x))}{A(t_o)} \right|^2 = 2 t_o \int_0^x \mathrm{Im}(\Delta\Omega)\, dx$$
$$= 2\sqrt{2}\, \omega_{MW} \hat{\sigma}_\tau F(x) , \tag{4.4}$$

where $\omega_{MW}/2\pi$ is the microwave frequency and

$$F(x) = \int_0^x \frac{\mathrm{Im}(u)}{1+x}\, dx , \tag{4.5}$$

which is plotted in Figure 5. We see that F(x) has a turning point at $x = 2.25$ where its slope 0.2194 is at a maximum and varies very slowly. In Figure 1(a), we see that

the power growth has a maximum slope of ~0.154 $msec^{-1}$ at ~65 msec after start of debunching. This implies that t_o ~65/(1+2.25) = 20.0 msec. However, the slope at 20.0 msec is ~-0.052 $msec^{-1}$. Thus the maximum slope should have been ~0.206 $msec^{-1}$ instead. With $\omega_{MW}/2\pi$ = 1.646 GHz and $\hat{\sigma}_T$ = 0.635 nsec, Eqs. (4.4) and (4.5) give a theoretical maximum slope of $4.075/t_o$ = 0.204 $msec^{-1}$ with t_o = 20 msec. Because of such a nice agreement, we take t_o ~20 msec. With $\hat{\sigma}_E$ = 0.0192 GeV and N = 0.636×10^{10}, we obtain Z/n = 8.63 Ω through Eq. (4.3).

V. OVERLAPPING

If we regard the half length of the bunch as $\sqrt{6}\sigma_T$, from Figure 6 and Eq. (A.2) in Appendix A, two adjacent bunches start touching each other when

$$t = \frac{\pi}{\eta \omega_{RF}(\sqrt{6}\,\hat{\sigma}_E/E)} = 10.7 \text{ msec} \tag{5.1}$$

after the RF is turned off. In above, $\omega_{RF}/2\pi$ is the RF frequency (~53.1 MHz). The growth of the microwave amplitude begins when t_o ≈20 msec or when two adjacent bunches completely overlap each other. As overlap occurs, one may expect the bunch becomes more stable because the energy spread σ_E which is small before overlap suddenly increases to the order of magnitude $\hat{\sigma}_E$, the value before

debunching. On the other hand, the overlapped bunches have a higher local peak current which therefore makes the bunch less stable. This problem is examined in detail in Appendix B, where we find that, as long as

$$\left(\frac{\sigma_E}{\Delta E}\right)^2 \ll 1 \,, \tag{5.2}$$

where ΔE is the energy difference between the overlapped bunches at some position, the stability criterion is still governed by σ_E; i.e.,

$$\frac{Z}{n} \leq (1.434)\,\frac{2\pi\eta\,(E/e)}{I_p}\left(\frac{\sigma_E}{E}\right)^2 \tag{5.3}$$

with I_p equal to the larger of the local peak currents of <u>one</u> of the bunches. As shown in Appendix A, the sheared bunch remains Gaussian, the peak current still occurs at the center of the bunch. In other words, the stability condition is exactly the same as that of a single bunch.

The threshold curve is plotted in the stability diagram in Figure 6(a). As $\mathrm{Re}(\Delta\Omega/n)$ increases from $-\infty$ to $+\infty$, the curve wraps around the origin twice (for two overlapped bunches). The threshold of Eq. (5.2) corresponds to point B where the driving impedance is real. Point C corresponds to Eq. (5.3) with the factor 1.434 reduced to

unity. This is the situation when Z/n is capacitive (above transition) and $Re(\Delta\Omega/n) \sim \pm$ half of the difference in revolution frequencies of the two overlapped bunches[4]. Point A is when $Re(\Delta\Omega/n) \sim 0$ and Z/n inductive[4]. This point actually corresponds to the ΔE, the difference in energies of the two bunches, and is $(\Delta E/2\sqrt{2}\sigma_E)^2$ away from the origin relative to point C. The threshold curve for one bunch is plotted in Figure 6(b) for comparison. Note that the positions of point B and C in two threshold curves are very nearly the same, although for one bunch, point C corresponds to $Re(\Delta\Omega/n) = 0$ instead. Usually point C is selected in a stability criterion, (sometimes point B if Z/n is definitely real). Therefore, for overlapped bunches, we have exactly the same criterion with I_p equal to the peak current of just one bunch.

For our experiment,

$$\frac{\sigma_E}{\Delta E} \approx \frac{\hat{\sigma}_\tau}{\Delta\tau} = 0.034$$

independent of time once overlap occurs. In above $\Delta\tau = 9.4$ nsec is the length of the half stationary bucket. Thus the condition (5.2) is satisfied and the stability criterion (5.3) is valid. So the broad band impedance driving the growth at 1.646 GHz is still $Z/n = 8.63\ \Omega$.

When the driving impedance exists as a high-Q resonance narrower than the spectrum spread of a bunch, the bunch will see only an effective impedance, the Z that appears in Eq. (5.3), depending on the length of the bunch. When the microwave signal starts to grow, the RMS bunch length is

$$\sigma_\tau = \frac{\eta \hat{\sigma}_E t_0}{E} \approx 7.18 \ nsec. \tag{5.4}$$

Thus, the high-Q resonance that we are talking about has a quality factor

$$Q \gtrsim \frac{\pi \omega_{MW} \sigma_\tau}{2\sqrt{2\pi}} \approx 47. \tag{5.5}$$

For a narrow resonance, a more meaningful parameter to quote is Z_{sh}/Q which is independent of the bunch length. For the growth to beat Landau damping, we must have[5]

$$\frac{Z_{sh}}{Q} \gtrsim (1.434) \frac{4\eta(E/e)}{I_{AV}} \left(\frac{\sigma_E}{E}\right)^2,$$

where I_{AV} is the average current of one bunch and the factor 1.434 comes about because the shunt impedance Z_{sh} is real. The experimental results indicate a narrow resonance of $Z_{sh}/Q = 6.37$ kΩ at 1.646 GHz in the Main Ring.

VI. DISCUSSIONS

(1) The longitudinal impedance per harmonic Z/n of the Main Ring has been estimated[6]. There does not appear to be any broad band around and above 1 GHz with Z/n = 8.6 Ω. Thus, the driving impedance of the growth in this experiment must come from some narrow resonances. There are quite a lot of narrow resonances in the 1.6 GHz region. These include the resonances of the bellows and beam monitors. For example, there is a bellow resonance of Z_{sh}/Q ~2.4 kΩ at 1.6 GHz according to the crude estimation of Reference 6, and also a monitor resonance of Z_{sh}/Q ~6.4 kΩ at 1.28 GHz. Also the pickup of this experiment has a peak response at ~1.5 GHz. All these can be the source of the driving force.

(2) There are things in the experiment that we do not understand. As soon as the RF is turned off, the amplitude should drop exponentially. However, we can see an increase from the exponential right from the start according to Figure 1(a). But we do not believe microwave instability starts immediately as the RF is turned off. Also, the microwave amplitude grows to a maximum value roughly equal to that before the RF is turned off. This is another mystery that we cannot explain. As a result, we should not believe so much in t_o ~ 20 msec, the time when the growth begins. It appears that this time is definitely less than

30 msec; but it is possible that it is something in between. A change in t_o will affect the value of Z/n or Z_{sh}/Q computed in Sections IV and V.

APPENDIX A

In the longitudinal phase space, if we let x represent the time τ relative to a synchronized particle and y = $\Delta E\hat{\sigma}_\tau/\hat{\sigma}_E$ the normalized energy spread, the contour enclosing 95% of the bunch becomes a circle. At time t, this circle becomes a elongated cigar as shown in Figure 7. Any particle with energy y will be ahead of the synchronized particle by an extra

$$\Delta\tau = \frac{\Delta\omega_o}{\omega_o} t \approx \eta t \frac{y\hat{\sigma}_E}{\hat{\sigma}_\tau E}, \tag{A.1}$$

where $\omega_o/2\pi$ is the revolution frequency. The shear angle θ is therefore

$$\cot\theta = \frac{y}{\Delta\tau} = \frac{E\hat{\sigma}_\tau}{\eta\hat{\sigma}_E t}. \tag{A.2}$$

Thus every point at x becomes x-y/cotθ, and the distribution in phase space is

$$f(x,y)\,dx\,dy = \frac{1}{2\pi\hat{\sigma}_\tau} \exp\left\{-\left[(x-y/\cot\theta)^2 + y^2\right]/2\hat{\sigma}_\tau^2\right\} dx\,dy, \tag{A.3}$$

which can be written as

$$f(x,y)\,dx\,dy = \frac{1}{\sqrt{2\pi}\,\hat{\sigma}_\tau \cos\theta} \exp\left[-(y - x\cos\theta\sin\theta)^2/2\hat{\sigma}_\tau^2\cos^2\theta\right] * \tag{A.4}$$

$$* \frac{\cos\theta}{\sqrt{2\pi}\,\hat{\sigma}_\tau} \exp\left[-x^2\cos^2\theta/2\hat{\sigma}_\tau^2\right] dx\,dy\,.$$

We see that the sheared bunch remains Gaussian. The instantaneous RMS energy spread and bunch length can be read off from Eq. (A.4):

$$\sigma_E = \hat{\sigma}_E \cos\theta\,, \tag{A.5}$$

$$\sigma_\tau = \hat{\sigma}_\tau / \cos\theta\,. \tag{A.6}$$

We note that when instability begins or $t = t_o$ ~20 msec, Eq. (A.2) gives $\cot\theta$ ~0.089 or θ very near to $\pi/2$. As a result, in Eqs. (A.5) and (A.6), $\cos\theta$ can be replaced by $\cot\theta$.

The coherent shift in microwave frequency $\Delta\Omega$ at time t is given by the dispersion relation

$$1 = -\left(\frac{\Delta\Omega_0}{n}\right)^2 \int \frac{F'(\omega)}{\Delta\Omega/n - \omega}\, d\omega\,, \tag{A.7}$$

where

$$F(\omega) = \frac{1}{\sqrt{2\pi}\,\sigma_\omega}\, e^{-\omega^2/2\sigma_\omega^2} \tag{A.8}$$

is the revolution frequency distribution of the bunch derived from Eq. (A.4) with the RMS frequency spread given by

$$\sigma_\omega = \frac{\eta \omega_0 \sigma_E}{\beta^2 E} . \tag{A.9}$$

By equating $F(\omega)$ to a δ-function, it is clear that $\Delta\Omega_0$ is the frequency shift without Landau damping. It is related to the driving impedance Z/n by

$$\left(\frac{\Delta\Omega_0}{n}\right)^2 = i \frac{e \eta \omega_0^2 I_p}{2\pi\beta^2 E} \frac{Z}{n} , \tag{A.10}$$

where $I_p = eN/\sqrt{2\pi}\sigma_T$ is the peak current of the bunch and β the velocity relative to that of light. Putting

$$u = \frac{\Delta\Omega}{\sqrt{2}\, n \sigma_\omega} , \tag{A.11}$$

The dispersion relation (A.7) can be simplified to

$$1 = -\frac{1}{2}\left(\frac{\Delta\Omega_0}{n\sigma_\omega}\right)^2 \int \frac{G'(z)}{u - z}\, dz \tag{A.12}$$

with

$$G(z) = \pi^{-\frac{1}{2}} e^{-z^2} . \tag{A.13}$$

At time $t = t_o(1+x)$, the integral in Eq. (A.12) can be carried out in terms of the complex error function w(u), giving

$$1 = -ia(1+x)\left[1 - i\sqrt{\pi}\,u\,W^*(u)\right], \tag{A.14}$$

where

$$a = \left(\frac{\Delta\Omega_o}{n\sigma_\omega}\right)^2_{t=t_o} = \frac{Z}{n}\frac{eNt_o}{(2\pi)^{3/2}\hat{\sigma}_\tau^2\hat{\sigma}_E} \cdot \tag{A.15}$$

Use has been made of Eqs. (A.2), (A.5), (A.6) and (A.9). When x<<1 or a short time after the growth has started, the integrated growth F(x) defined in Eq. (4.5) is

$$F(x) = (0.5181)\left[\ln(1+x) - \frac{x}{1+x}\right] \cdot \tag{A.16}$$

However, the maximum slope of F(x) occurs at a point where x is not small. Thus, exact numerical solution of Eq. (A.14) is necessary. The exact F(x) is plotted in Figure 5.

APPENDIX B

We start from the dispersion relation (A.7)

$$1 = -\left(\frac{\Delta\Omega_o}{n}\right)^2 \int \frac{F'(\omega)}{\Delta\Omega/n - \omega}\, d\omega . \tag{B.1}$$

The current I_T in

$$\left(\frac{\Delta\Omega_0}{n}\right)^2 = i\,\frac{e\eta\omega_0^2 I_T}{2\pi\beta^2 E}\,\frac{Z}{n} \tag{B.2}$$

is

$$I_T = I_1 + I_2\,, \tag{B.3}$$

the sum of the local currents of the first and second bunches at some location in the overlap. There, the revolution frequency distribution is

$$F(\omega) = \frac{1}{\sqrt{2\pi}\,\sigma_\omega}\left[\alpha_1 e^{-(\omega-\omega_1)^2/2\sigma_\omega^2} + \alpha_2 e^{-(\omega-\omega_2)^2/2\sigma_\omega^2}\right], \tag{B.4}$$

where ω_1 and ω_2 are respectively the mean deviations of revolution frequencies of the bunches from that of the synchronized particle. Here, we consider $\omega_1<0$ amd $\omega_2>0$, so that the mean difference in revolution frequencies is $\Delta\omega = \omega_2+|\omega_1|$. We also assume

$$\left(\frac{2\sqrt{2}\,\sigma_\omega}{\Delta\omega}\right)^2 \ll 1\ . \tag{B.5}$$

The parameters

$$\alpha_1 = \frac{I_1}{I_1 + I_2} \qquad and \qquad \alpha_2 = \frac{I_2}{I_1 + I_2} \tag{B.6}$$

represent the fractional contributions of the bunches and $F(\omega)$ is clearly normalized to unity.

Let us consider the case when Z/n is imaginary; i.e., $(\Delta\Omega_o/n)^2$ is real. Then, the thresholds are given by

$$1 = -\left(\frac{\Delta\Omega_o}{n}\right)^2 \mathcal{P}\int \frac{F'(\omega)}{\Delta\Omega/n - \omega}\, d\omega, \tag{B.7}$$

where $\Delta\Omega/n$ are the zeros of $F'(\omega)$. From Figure 7, we see that there are three zeros: $(\Delta\Omega/n)_1 \sim \omega_1$, $(\Delta\Omega/n)_2 \sim \omega_2$ and $(\Delta\Omega/n)_3$ in between. With $(\Delta\Omega/n)_1$, say, the integral in Eq. (B.7) receives contribution nearly entirely from the bunch at ω_1 because of Eq. (B.5). Thus, the threshold criterion derived from this zero should correspond to the bunch at ω_1 only and is therefore determined by σ_ω (or σ_E). The principal value of the integral is positive and therefore $(\Delta\Omega_o/n)^2$ is negative corresponding to point C of the threshold curve of Figure 6. In the same manner, the zero $(\Delta\Omega/n)_2 \sim \omega_2$ will lead to contribution mostly from the bunch at ω_2. Therefore, this also corresponds to point C. As for the third zero, the principal value of the integral is negative. Since $(\Delta\Omega/n)_3$ is far away from both bunches, this principal value is small also. If we let $\alpha_1 = \alpha_2 = 1/2$ and $|\omega_1| = \omega_2$, $(\Delta\Omega/n)_3 = 0$, then $(\Delta\Omega_o/n)^2 \sim (\Delta\omega)^2/4$ which corresponds to point A in Figure 6. All the above

discussions hold for any frequency distribution for $F(\omega)$ with two narrow but widely separated humps.

If we take the Gaussian distribution of Eq. (B.4) seriously, the threshold curve can be solved exactly. From Eq. (B.1) at threshold, we get

$$\left(\frac{\Delta\Omega_0}{n}\right)^{-2} = -\frac{1}{\sigma_\omega^2}\left[1 - i\alpha_1\sqrt{\pi}\,u_1 W^*(u_1) - i\alpha_2\sqrt{\pi}\,u_2 W^*(u_2)\right] \tag{B.9}$$

where

$$\begin{aligned} u_1 &= \frac{\Delta\Omega}{\sqrt{2}\,n\sigma_\omega} - \frac{\omega_1}{\sqrt{2}\,\sigma_\omega}\,, \\ u_2 &= \frac{\Delta\Omega}{\sqrt{2}\,n\sigma_\omega} - \frac{\omega_2}{\sqrt{2}\,\sigma_\omega}\,, \end{aligned} \tag{B.10}$$

and w(u) is the complex error function. At $u_1 = 0$,

$$\left(\frac{\Delta\Omega_0}{n}\right)^{-2} = -\frac{1}{\sigma_\omega^2}\left[1 - 2\alpha_2\frac{\Delta\omega}{\sqrt{2}\sigma_\omega}e^{-\left(\frac{\Delta\omega}{\sqrt{2}\sigma_\omega}\right)^2}\int_0^{\frac{\Delta\omega}{\sqrt{2}\sigma_\omega}} e^{t^2}dt\right]. \tag{B.11}$$

When $(\Delta\Omega/\sqrt{2}\sigma_\omega)^2 >> 1$, this becomes

$$\begin{aligned} \left(\frac{\Delta\Omega_0}{n}\right)^{-2} &= -\frac{1}{\sigma_\omega^2}\left\{1 - \alpha_2\left[1 + \left(\frac{\sigma_\omega}{\Delta\omega}\right)^2\right]\right\} \\ &= -\frac{\alpha_1}{\sigma_\omega^2} + \frac{\alpha_2}{(\Delta\omega)^2}\,. \end{aligned} \tag{B.12}$$

Similarly, at $u_2 = 0$

$$\left(\frac{\Delta\Omega_0}{n}\right)^{-2} = -\frac{\alpha_2}{\sigma_\omega^2} + \frac{\alpha_1}{(\Delta\omega)^2} \cdot \tag{B.13}$$

For the third zero, taking $\alpha_1 = \alpha_2$,

$$\left(\frac{\Delta\Omega_0}{n}\right)^{-2} = \frac{4}{(\Delta\omega)^2} \cdot \tag{B.14}$$

The threshold criterions of Eq. (B.12) and (B.13) are obviously more stringent than that of Eq. (B.14). Taking Eq. (B.12) and neglecting the $(\Delta\omega)^{-2}$ term, we get using Eq. (B.2),

$$i\,\frac{e\eta\omega_0^2 I_T}{2\pi\beta^2 E}\frac{Z}{n} = -\frac{\sigma_\omega^2}{\alpha_1} \cdot \tag{B.15}$$

Noting the definitions of I_T and α_1 in Eqs. (B.3) and (B.6) and also the relation between σ_ω and σ_E in Eq. (A.9), we arrive at

$$\frac{Z}{n} = i\,\frac{2\pi\eta(E/e)}{I_1}\left(\frac{\sigma_E}{E}\right)^2, \tag{B.16}$$

which is just the threshold condition for the first bunch since the local current I_1 for the first bunch appears in the formula. Using Eq. (B.13), we get exactly the same threshold as Eq. (B.16) with the only exception that I_2 appears instead of I_1. Because according to Eq. (A.3) the

sheared bunch remains Gaussian both in time spread and energy spread, the peak local current is again at the center of the bunch. Thus, in Eq. (B.16) for the limit of Z/n, we should put $I_1 = eN/\sqrt{2\pi}\sigma_\tau$. In other words, the threshold criterion for overlapped bunches is exactly the same as that for a single non-overlapping bunch. A typical threshold curve for two overlapped bunches with $\alpha_1 = \alpha_2$, $|\omega_1| = \omega_2$ and $(\omega_1/\sqrt{2}\sigma_\omega)^2 = 10$ is computed according to Eq. (B.9) and is plotted in Figure 7(a). We see that, near the origin, the threshold curve is nearly identical to the one for a single bunch plotted alongside in Figure 7(b). This is because the contribution to the first curve in that region comes mostly from only one bunch as is indicated in Eq. (B.12).

REFERENCES

1. J. Crisp, private communication
2. D. Boussard, CERN/LABII/RF/Int./75-2, 1975.
3. B.A. Prichard, J.E. Griffin, R.F. Stiening and E. Wilson, Fermilab EXP. 74, 1975.
4. Here we assume that we are at a point in the overlapped bunches where the intensity of each bunch is the same and the mean revolution frequency of each bunch deviates from that of the synchronized particle by the same amount. These conditions are relaxed in Appendix B.

5. This criterion can be proved easily if the resonance is assumed to be a δ-function without any imaginary part. However, causality will be violated.

6. K.Y. Ng, Fermilab Report TM-1388.

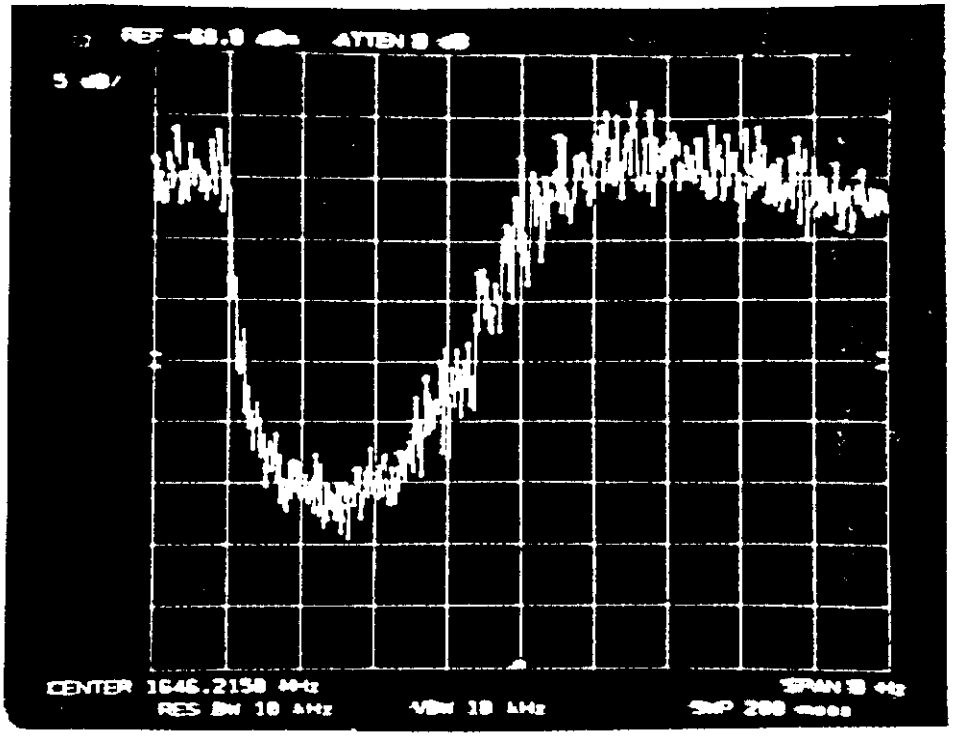

(a) Zero span mode 10 MHz bandwidth analyzer. Scales are 5db/div and 20ms/div.

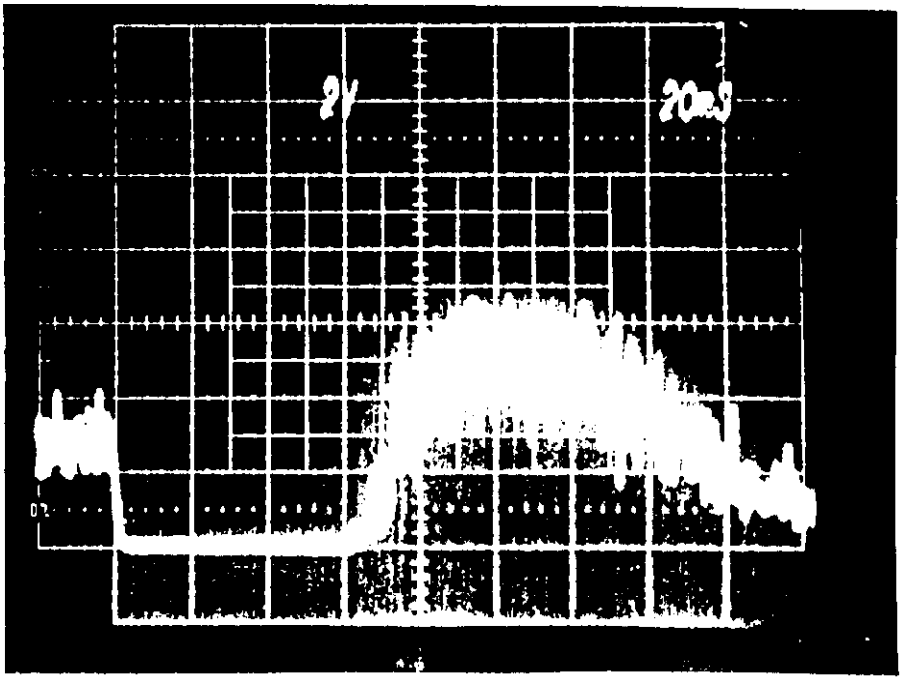

(b) Diode detector. Scales are 2V/div and 20ms/div.

Figure 1. Comparison of the starting growth times by zero-span analyzer and diode detector

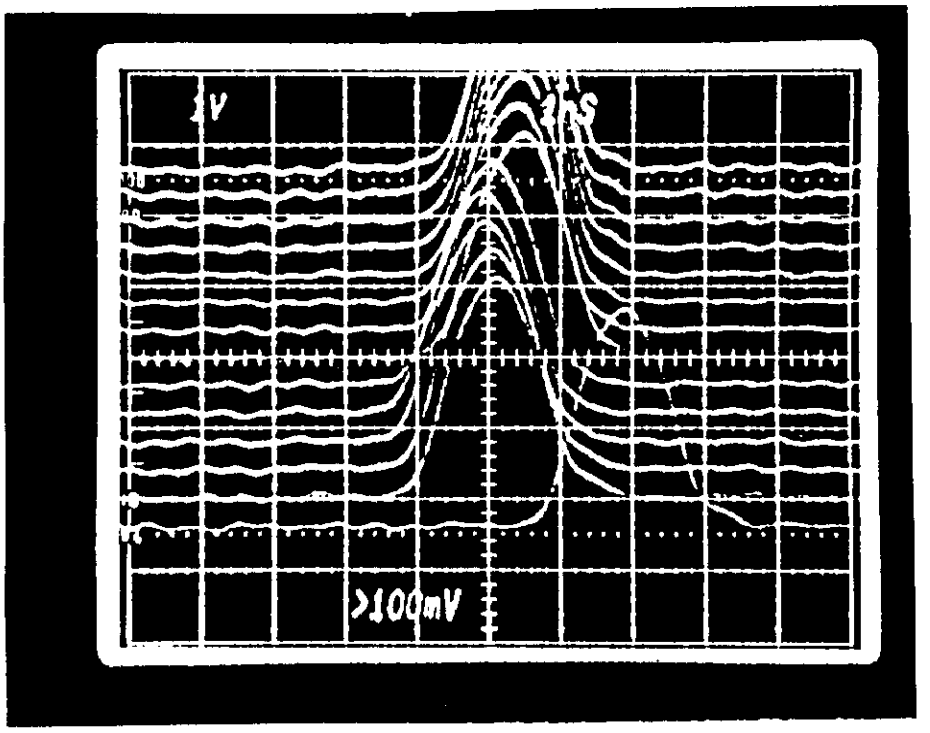

Figure 2. Bunch shape before RF turn off.

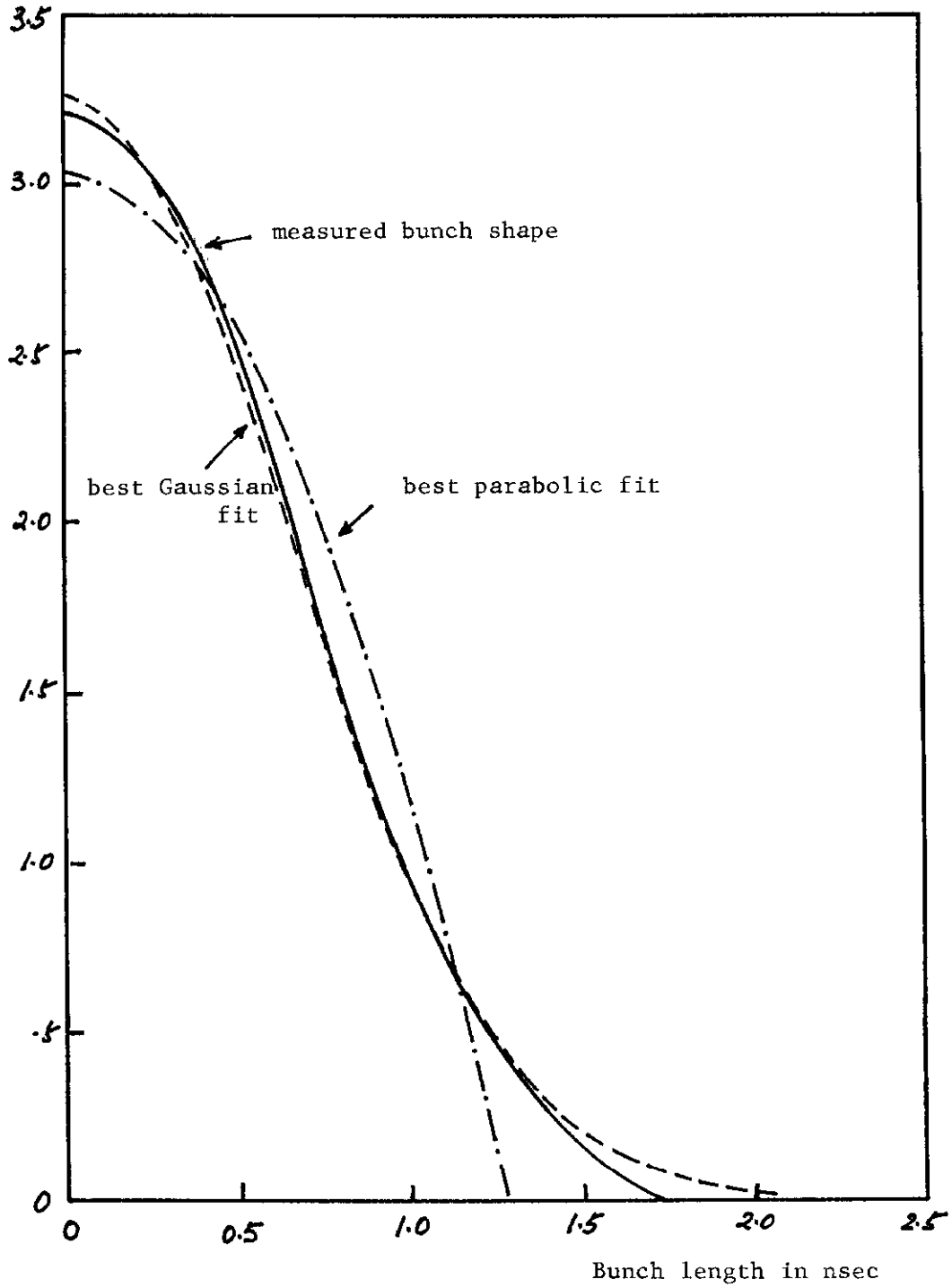

Figure 3. Bunch shape fittings. Solid curve is the measured bunch shape. Dot-dashed curve is the best parabolic fit with half bunch length = 1.278 nsec. Dashed curve is the best Gaussian fit with RMS time spread $\hat{\sigma}_z = 0.635$ nsec.

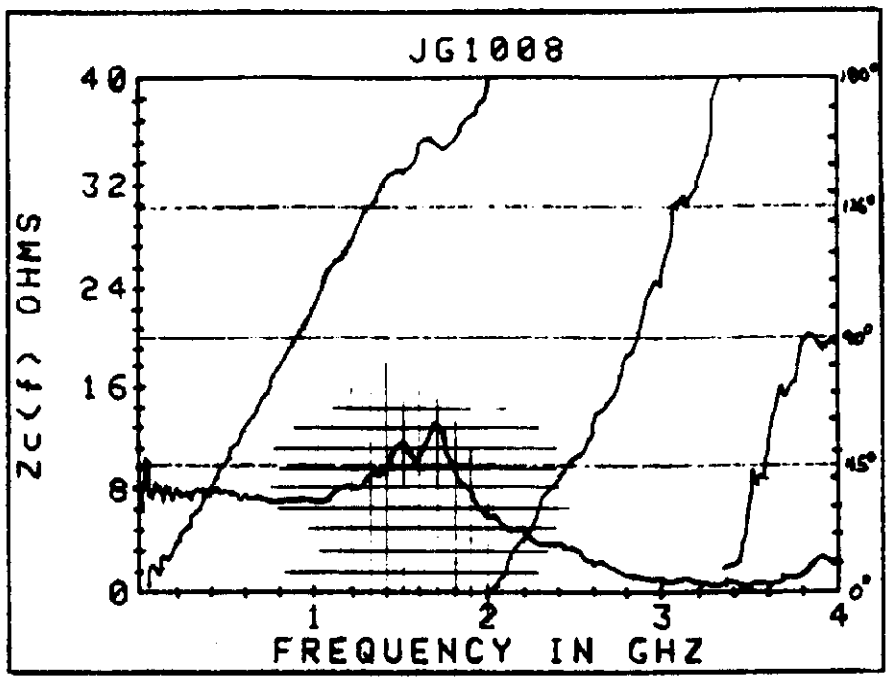

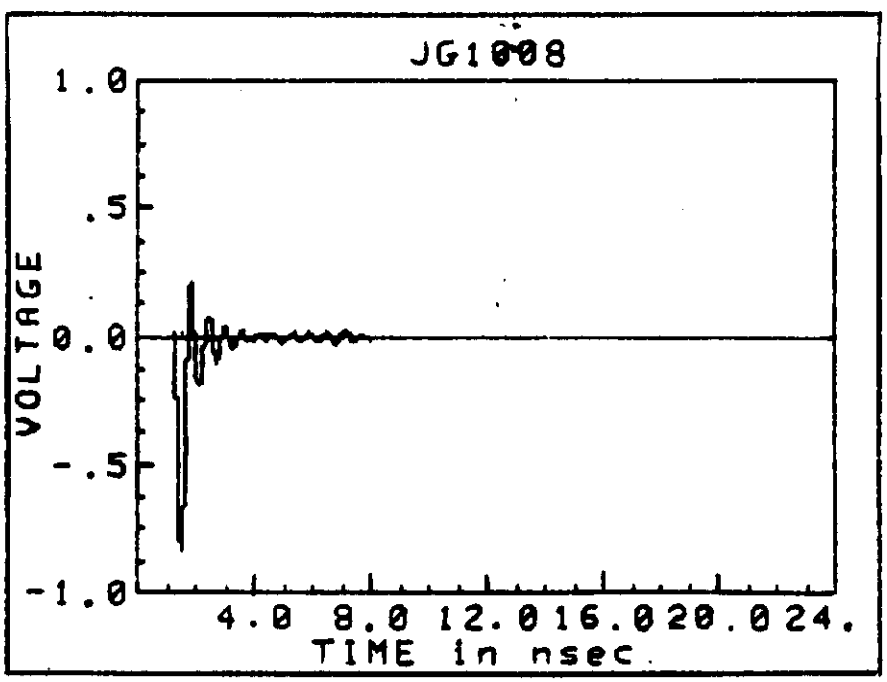

Figure 4. Time and frequency domain response of detector to 30 psec electron bunch at Argonne National Laboratory.

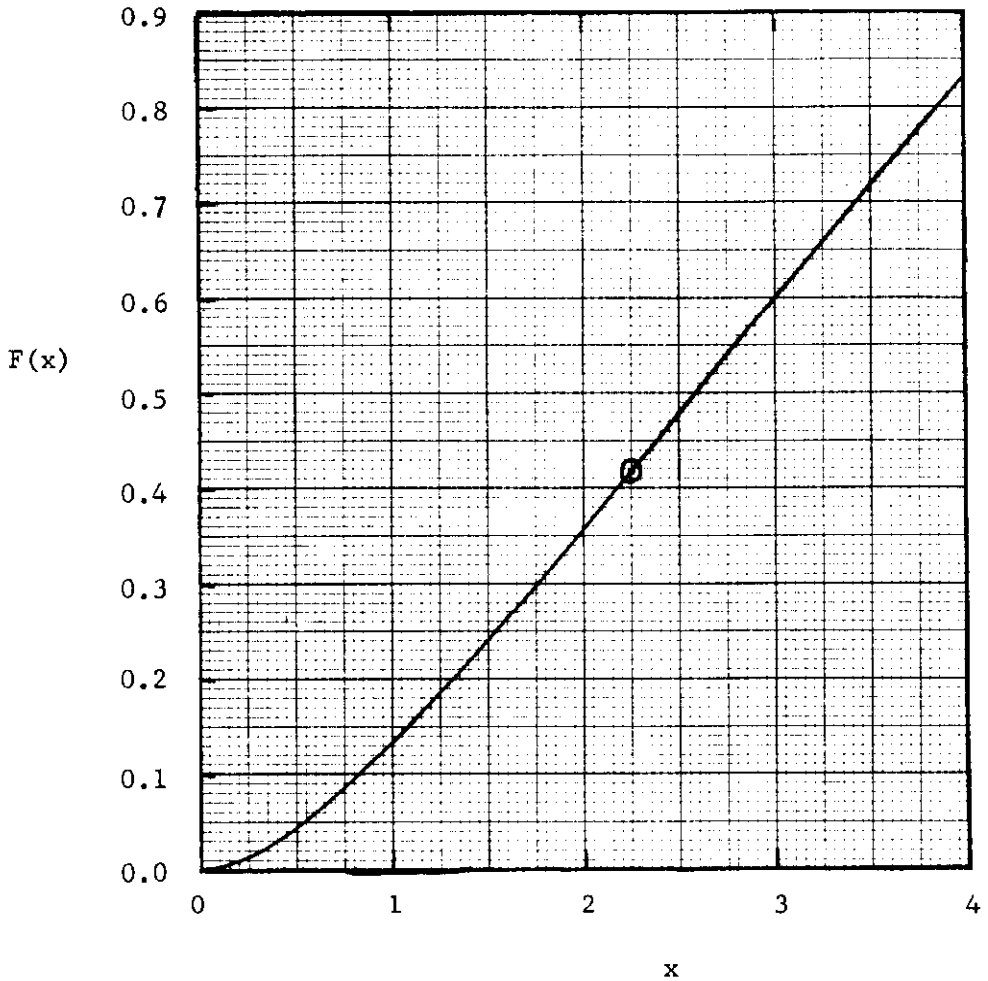

Figure 5. The normalized integrated growth rate F(x) of Eq. (4.5). The turning point is at $x = 2.25$ where the slope is 0.2194 .

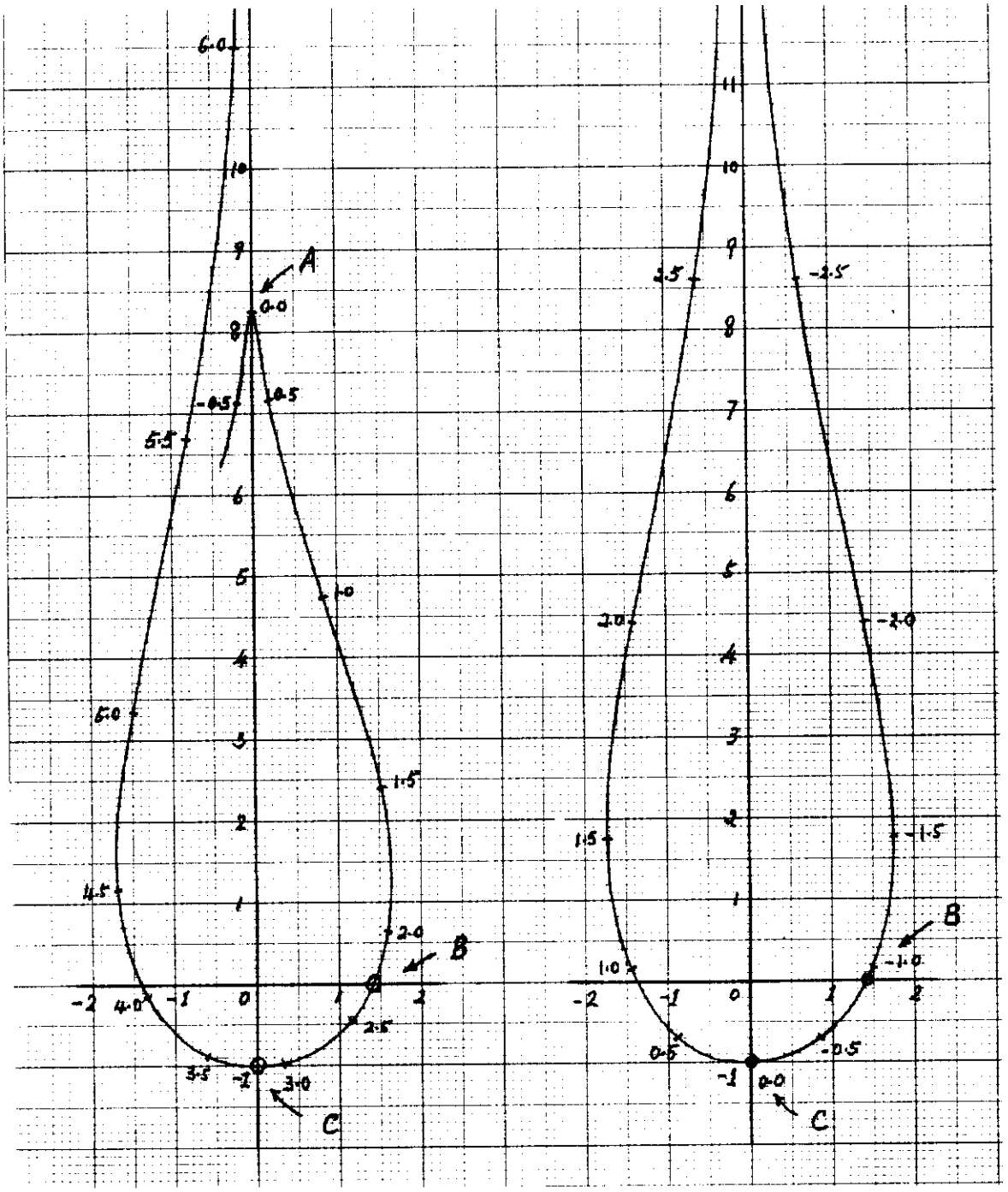

Figure 6. Threshold curves for (a) two overlapped bunches and (b) a single bunch. In each case, the abscissa and ordinate are the real and imaginary parts of $(\Delta\Omega_o/n\sigma_\omega)^2$ respectively. The real coherent frequency shift $\mathcal{R}e(\Delta\Omega/\sqrt{2}n\sigma_\omega)$ is marked along the curves. For (a), because of clarity, only half of the curve is plotted. We have taken $\alpha_1 = \alpha_2$, $|\omega_1| = \omega_2$, and $(\omega_1/\sqrt{2}\sigma_\omega)^2 = 10$ (see Appendix B).

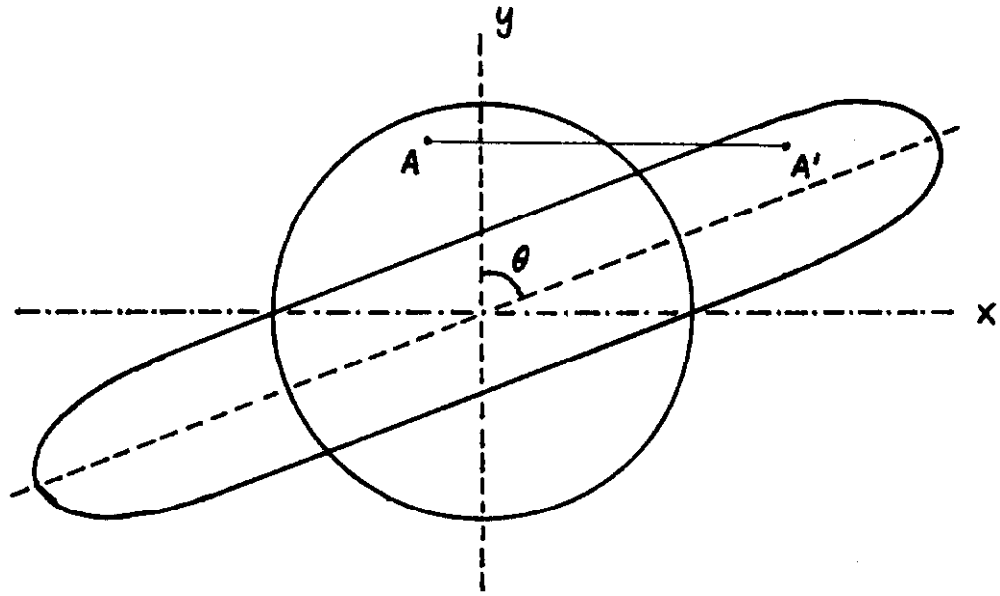

Figure 7. The sheared bunch. The point A goes to A'. Length of AA' $= y \tan\theta$, where θ is the shear angle.